

# Kinetics Study and Modelling of the Steam Methane Reforming Reaction for Hydrogen Production

\*Yiga, F.; Dagde, K.K.; Akpa, J.G.; Ikenyiri, P.N.

Chemical/Petrochemical Engineering Department, Rivers State University, Port Harcourt-Nigeria

\*Corresponding Author: yiga.francis@ust.edu.ng

**Abstract**—A kinetic model for the steam methane reforming (SMR) reaction to produce hydrogen was developed using the Langmuir-Hinshelwood (LH) approach. The kinetics model incorporated the competitive adsorption and reaction of  $\text{CH}_4$  and  $\text{H}_2\text{O}$  on nickel-based catalyst active sites to produce hydrogen and carbon dioxide. The model was solved using MATLAB and was validated against experimental data. The model predicted a methane fractional conversion of 0.94 after 20 minutes which agreed closely with the experimental value of 0.93 fractional conversion after 20 minutes, with RMSE values of 0.01. Sensitivity analysis studies showed that increasing steam-to-carbon ratio (S/C) from 1 to 4 increased the final conversion from 0.50 to 0.96 after 2000s, with S/C = 3 offered an optimal conversion of 0.93. Temperature elevation from 700 to 900 °C accelerated conversion significantly, reaching 0.95 within 1000s at 900 °C. The simplified rate expression is computationally efficient and suitable for reactor design and dynamic control studies, providing a practical tool for hydrogen production process optimisation.

**Keywords**—Conversion, Kinetics model, Reaction, Reforming, and simulation.

## I. INTRODUCTION

The Rising global energy demand is driven by population growth, industrialisation, and technological advancement. Fossil fuels such as coal, oil, and natural gas continue to supply most of world energy, yet their combustion releases large volumes of greenhouse gases, particularly  $\text{CO}_2$ , which is a leading cause of climate change Massarwehet et al. (2023).

In response, international climate pledges and decarbonisation strategies have sped up the move towards renewable and low-carbon energy systems. Despite the growing share of solar, wind, biomass, and geothermal power, their unpredictable and fluctuating nature poses difficulties for maintaining a stable energy supply Ishaq et al. (2019).

Hydrogen has gained prominence as a strategic energy carrier due to its high energy density per unit mass, versatility across industrial sectors, and emission-free combustion Staffell et al. (2024). Hydrogen combustion produces only water vapour, making it an environmentally clean fuel Bayramoglu et al. (2024). These features allow hydrogen to be used in transport, energy storage, electricity generation, steel production, and the chemical industry Muhammed et al. (2023). Hence, hydrogen acts not only as a fuel but also as an energy vector that connects different parts of the energy system Bilgili (2023).

The SMR process involves two principal reactions: the highly endothermic steam reforming reaction and the moderately exothermic water-gas shift reaction. Both reactions are reversible and typically occur over nickel-based catalysts at

elevated temperatures between 700 and 1000 °C (Rostrup-Nielsen & Sehested, (2002). However, the SMR process is highly sensitive to variations in temperature, pressure, and feed composition, making accurate kinetic modeling essential for reliable reactor design, performance prediction, and process optimization.

The development of a robust kinetic model for SMR has been a long-standing challenge. The Langmuir-Hinshelwood framework is widely adopted to describe catalytic surface reactions, as it accounts for the competitive adsorption of reactants and products on catalyst active sites. Over the years, several researchers have contributed to the understanding of SMR kinetics under various conditions.

Zeppieri et al. (2010) investigated the kinetics of methane steam reforming over commercial nickel-based and innovative rhodium-perovskite catalysts using a lab-scale micro-reactor at 723–1023 K and atmospheric pressure. They applied the Wei and Iglesia kinetic model, assuming methane activation as the rate-determining step. The results showed that the rhodium-perovskite catalyst exhibited higher activity, achieving methane conversions closer to equilibrium with lower carbon deposition and a lower activation energy (69.1 kJ/mol) compared to the nickel catalyst (96.1 kJ/mol). Although the model showed good agreement with experimental data, the study was limited to atmospheric pressure, which does not fully represent industrial SMR conditions.

Mbodji et al. (2012) developed a detailed experimental and numerical model for SMR intensification using a millistructured reactor with a rhodium-based catalyst under industrial conditions (800–900 °C and 20 bar) and a steam-to-carbon ratio of 3. Their plug-flow reactor model, which accounted for heat and mass transfer, accurately predicted methane conversion (86–99%) and outlet temperature. However, the study assumed steady-state operation and focused on a specific reactor configuration, limiting the generalizability of the kinetic parameters to conventional packed-bed reformers.

Stoppacher et al. (2023) examined catalyst deactivation in SMR within chemical looping hydrogen systems, focusing on the effects of hydrogen sulfide contamination (1–10 ppm) on nickel-based catalysts. They developed a one-dimensional plug-flow reactor model and found that higher  $\text{H}_2\text{S}$  concentrations increased deactivation rates and reduced methane conversion efficiency. While the work provides valuable insights into catalyst stability, it did not develop a generalized kinetic rate expression applicable across different operating conditions.

Avetisov et al. (2010) proposed and validated an advanced microkinetic model for both steam methane reforming and dry methane reforming over a nickel catalyst. The model explicitly accounted for pore-diffusion resistance and successfully explained phenomena such as the change in methane reaction order with pressure, the accelerating effect of steam, and the retardation by hydrogen. However, the complexity of the microkinetic model results in high computational demands, limiting its integration into real-time process simulation or control applications.

Nieva et al. (2014) investigated SMR at low temperatures (500–600 °C) by comparing four nickel-based catalysts prepared by impregnation and coprecipitation. It was found that the Ni-Zn-Al catalyst prepared by coprecipitation exhibited the highest activity and stability, inhibiting filamentary carbon formation. The study focused on catalyst formulation.

Moreira et al. (2013) developed a methodology to obtain the kinetic mechanism of SMR in a compact reactor using computational fluid dynamics coupled with a hybrid genetic surface response optimization. A multi-objective genetic algorithm was applied to optimize six kinetic parameters. Although the approach improved kinetic parameter accuracy, it requires high computational resources, which restricts its application in reactor design and real-time optimization.

Other studies have explored various aspects of SMR kinetics and reactor performance. Gokon et al. (2014) investigated solar-driven SMR with carbonate molten-salt absorber reformer tubes, focusing on thermal stability rather than intrinsic kinetics. Ganguli and Bhatt (2023) reviewed advanced reactor technologies for SMR, including membrane reactors, sorption-enhanced reactors, and microreactors, highlighting process intensification but not developing new kinetic models.

Dogo et al. (2022) developed a one-dimensional heterogeneous model for SMR over a nickel-based catalyst, validating the model against industrial data, but the study focused primarily on steady-state reactor predictions and did not address the derivation of a simplified, validated Langmuir-Hinshelwood rate expression.

From the review of these previous works, several important research gaps emerge. First, many kinetic studies were conducted at atmospheric pressure, which does not accurately represent industrial SMR operations that typically occur at elevated pressures (15–35 bar). Second, most existing models are either overly complex, requiring extensive computational resources, or are validated only under limited operating conditions. Third, there is a scarcity of simplified, physically meaningful Langmuir-Hinshelwood rate expressions that can be readily integrated into reactor-scale models and control system design. Finally, few studies have systematically derived and validated a rate expression that focuses on the forward reaction under high-temperature conditions where product partial pressures are initially low.

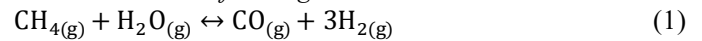
To address these gaps, the present study develops a rate expression model for the steam methane reforming reaction using the Langmuir-Hinshelwood approach, with a specific focus on forward reaction kinetics under the influence of a nickel-based catalyst. The model is derived from first

principles, incorporating the competitive adsorption of methane and steam on catalyst active sites, and is subsequently simplified under high-temperature operating conditions where product partial pressures are negligible.

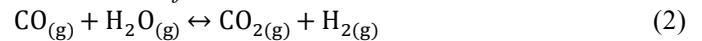
## II. MATERIALS AND METHODS

The development of the reaction kinetics follows the Langmuir-Hinshelwood (LH) approach. The approach establishes the relationship between mono-layer species adsorption to surface reaction on the surface of the catalyst active sites at equilibrium. The reaction taking place consists of two series reaction: steam-methane reforming (SMR) reaction and water-gas-shift reaction (WGS).

*Steam Methane Reforming Reaction*

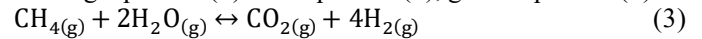


*Water Gas Shift Reaction*



*Global Reaction*

Adding equation (1) and equation (2), gives equation (3)

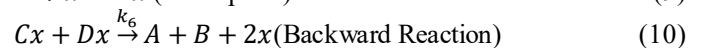
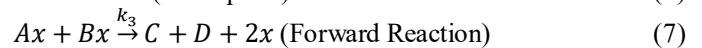
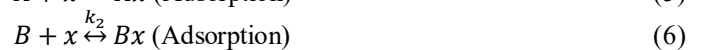
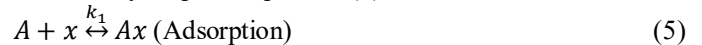


Let A = CH<sub>4</sub>; B = H<sub>2</sub>O; C = CO<sub>2</sub> and D = H<sub>2</sub>

The langmuir-Hinshelwood kinetic approach was employed in the development of the kinetic model for steam-methane reforming process as follows:



Elementary steps of equation (4) reaction mechanism



The generalized L-H rate expression is given as:

$$r = \frac{k \cdot \text{Driving Force}}{(1 + \sum K_i P_i)^n} \quad (11)$$

*Site Balance*

$$\sum \theta_i + \theta_x = 1 \quad (12)$$

$$-r_A = \frac{k_3 K_A P_A K_B P_B - k_6 K_C P_C K_D P_D}{(1 + K_A P_A + K_B P_B + K_C P_C + K_D P_D)^2} \quad (13)$$

$$\sum y_i = 1 \quad (14)$$

$$y_A = y_{A0} (1 - X_A) \quad (15)$$

$$M = \frac{y_{A0}}{y_{B0}} \quad (16)$$

$$y_B = y_{B0} (1 - 2MX_A) \quad (17)$$

SMR is operated at 850–950 °C, high operating temperature drives the reaction forward which According to Le Chatelier's Principle, high temperature shifts equilibrium toward products. So, product concentrations are initially low, especially at the reactor inlet, meaning

$$-r_A = k P^2 y_A y_B \quad (18)$$

$$-r_A = k P^2 y_{A0} y_{B0} (1 - X_A) (1 - 2MX_A) \quad (19)$$

$$k = A \exp\left(-\frac{E_A}{RT}\right) \quad (20)$$

## III. RESULTS AND DISCUSSION

The kinetic model was solved using MATLAB, and the results are presented in table I, figures 1 and 2. The kinetic

model results were validated using experimental data contained in the literature (Abbas *et al.*, 2017).

TABLE I: Validation of SMR Kinetics Model Predictions against Experimental Data

| Parameter                                    | Model Value | Experimental Value | RMSE   |
|--|-------------|--------------------|--------|
| CH <sub>4</sub> Conversion $X_A$             | 0.94        | 0.93               | 0.01   |
| CH <sub>4</sub> Conc. (kmol/m <sup>3</sup> ) | 0.0044      | 0.0049             | 0.0005 |
| Steam Conc. (kmol/m <sup>3</sup> )           | 0.0771      | 0.0779             | 0.0008 |
| CO <sub>2</sub> Conc. (kmol/m <sup>3</sup> ) | 0.0639      | 0.0635             | 0.0055 |
| H <sub>2</sub> Conc. (kmol/m <sup>3</sup> )  | 0.2559      | 0.2542             | 0.0017 |

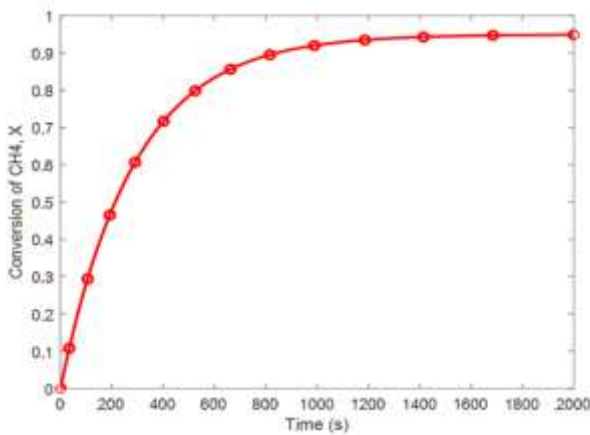


Fig. 1: Conversion Profile of Methane with Time

Fig. 1 showed the graph of conversion of methane in the steam-methane reforming (SMR) process. Conversion increased rapidly during the initial 0-400 seconds due to high reactant availability and strong driving force for the endothermic reaction, indicating full catalyst activity. Between 400-1000s, the rate of conversion followed an exponential increment as methane concentration decreased and equilibrium limitations became significant.

Beyond 1000s, the curve leveled off, stabilizing at 0.93, which represented the steady-state operating condition under the specified process parameters.

Fig. 2 illustrated the concentration profiles of methane (CH<sub>4</sub>), steam (H<sub>2</sub>O), hydrogen (H<sub>2</sub>) and carbon dioxide (CO<sub>2</sub>) in the SMR reactor over 2000s. Initially, CH<sub>4</sub> and H<sub>2</sub>O concentrations of 0.07kmol/m<sup>3</sup> and 0.25kmol/m<sup>3</sup> respectively, declined sharply due to the reforming and water-gas shift reactions. CH<sub>4</sub> concentration approached zero by 1000s, while H<sub>2</sub>O concentration depleted to about 0.1kmol/m<sup>3</sup>. In contrast, H<sub>2</sub> concentration increased steadily to 0.25kmol/m<sup>3</sup>, and CO<sub>2</sub> rose to 0.05kmol/m<sup>3</sup>, consistent with equilibrium constraints. The presence of residual H<sub>2</sub>O suggested that a steam-to-carbon ratio of 3 was optimal to prevent coke formation.

The fig. 3 illustrates the effect of steam-to-carbon (S/C) ratio on methane conversion over time at constant temperature and pressure. Higher S/C ratios significantly accelerate the conversion rate and increase the final conversion. For S/C = 1, conversion rises slowly to about 0.5 at 2000 s, indicating limited steam availability, this restricted the reforming reaction. As S/C increases to 2 and 3, conversion improve greatly,

reaching approximately 0.75 and 0.93, respectively. At S/C = 4, conversion approaches 0.96, at the expense of excessive dilution reducing process efficiency. Overall, S/C = 3 offers an optimal balance between high conversion and process efficiency

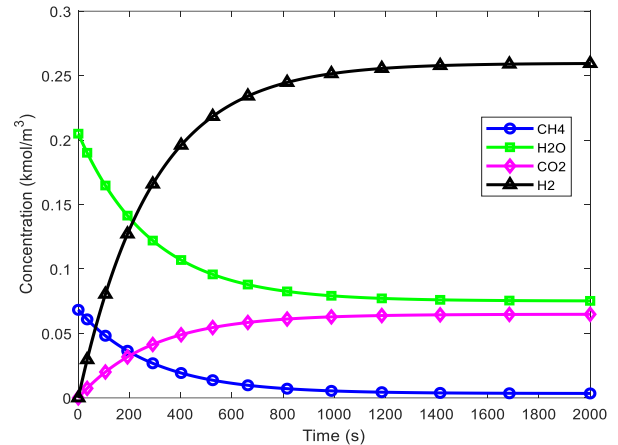


Fig. 2: Components Concentration Profile with Time

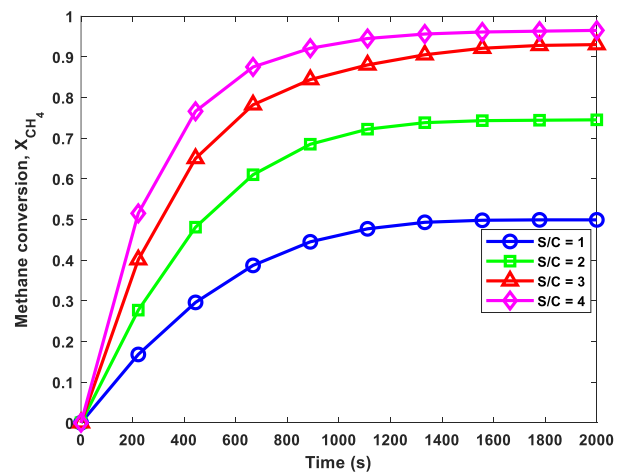


Fig. 3: Effect of steam-to-carbon (S/C) ratio on methane conversion over time

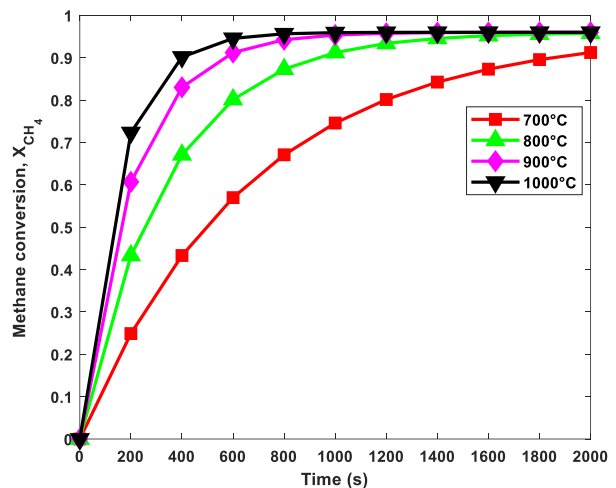


Fig. 4: Effect of temperature on methane conversion over time

Fig.4 demonstrated the strong temperature dependence of methane conversion over time. At 700 °C, conversion increases slowly, reaching only about 0.5 at 2000 s, due to the endothermic nature of steam methane reforming. At temperature of 800 °C conversion improve significantly, reaching 0.85. At 900 °C and 1000 °C, conversion exceeds 0.95 within 1000 s, indicating that high temperatures shift the equilibrium toward products and accelerate kinetics.

IV. CONCLUSION

A simplified Langmuir-Hinshelwood rate expression for the steam methane reforming reaction was successfully derived. The model achieved a methane conversion of 94%, closely matching the experimental value of 93%, with RMSE values below 0.01. Sensitivity analysis showed that increasing the steam-to-carbon ratio from 1 to 4 raises conversion from 0.50 to 0.96 after 2000 s, with S/C = 3 offering optimal performance at 93% conversion. Temperature elevation from 700 to 900 °C accelerates conversion, reaching 95% within 1000 s. The computationally efficient kinetic model is well-suited for reactor design, dynamic simulation, and process optimisation in hydrogen production.

NOMENCLATURE

| Symbols    | Descriptions  | Units                            |
|------------|---|----------------------------------|
| i          | Reaction species (A, B, C, and D)                         | -                                |
| r          | Reaction rate of steam methane reforming                  | $kmol \cdot m^{-3} \cdot s^{-1}$ |
| k          | Rate constant for surface reaction                        | $kmol \cdot m^{-3} \cdot s^{-1}$ |
| $k_3$      | Forward reaction rate constant                            | $kmol \cdot m^{-3} \cdot s^{-1}$ |
| $k_6$      | Backward reaction rate constant                           | $kmol \cdot m^{-3} \cdot s^{-1}$ |
| $K_i$      | Adsorption equilibrium constant for species (i)           | $bar^{-1}$                       |
| $P_i$      | Partial pressure of species (i)                           | bar                              |
| $\theta_i$ | Fraction of catalyst active sites occupied by species (i) | -                                |
| $\theta_x$ | Fraction of vacant (free) catalyst active sites           | -                                |
| x          | Active site on catalyst surface                           | -                                |
| $y_i$      | Mole fraction of species (i)                              | -                                |
| $X_A$      | Fractional conversion of species A                        | -                                |
| $X_B$      | Fractional conversion of species B                        | -                                |
| t          | Time  | s                                |
| T          | Temperature   | °C                               |
| P          | Total system pressure                                     | bar                              |
| R          | Universal gas constant                                    | $J \cdot mol^{-1} \cdot K^{-1}$  |
| $E_A$      | Activation energy   | $kJ \cdot mol^{-1}$              |
| $k_o$      | Pre-exponential factor                                    | -                                |
| S/C        | Steam-to-carbon ratio                                     | -                                |
| RMSE       | Root mean square error                                    | -                                |
| $C_i$      | Molar concentration of species (i)                        | $kmol \cdot m^{-3}$              |
| $F_i$      | Molar flow rate of species (i)                            | $kmol \cdot s^{-1}$              |

REFERENCES

- [1] M. Zeppieri, M. Raffaele, & A. Vaccari, (2010). Kinetics of methane steam reforming over nickel-based and rhodium-perovskite catalysts. *International Journal of Hydrogen Energy*, vol. 35 issue 13, pp. 6655–6664.
- [2] M. Mbodji, N. Abatzoglou, & D. Grouset, (2012). Steam methane reforming intensification using a millistructured reactor: Experimental and modeling study. *Chemical Engineering Journal*, 495–503.
- [3] P. Stoppacher, J. Schmid, & H. Hofbauer, (2023). Impact of hydrogen reforming on catalyst deactivation in chemical looping steam methane reforming. *Fuel*, 345, 128234.
- [4] A. Avetisov, O. Malykh, R., Gremadzki, L. M., Apelbaum, J. R., Rostrup-Nielsen, & V. S. Beskov, (2010). Steady-state kinetics and mechanism of methane reforming with steam and carbon dioxide over Ni catalyst. *Journal of Molecular Catalysis A: Chemical*, vol. 315, issue 2, pp. 170–178.
- [5] M. Nieva, M. Villaverde, & A. Monzón, (2014). Low-temperature steam reforming of methane over Ni-based catalysts: Effect of preparation method. *Applied Catalysis A: General*, 471, 73–83.
- [6] J. Moreira, A. Silva, & J. Figueiredo, (2013). Hybrid genetic algorithm and CFD approach for kinetic parameter estimation in methane steam reforming. *Chemical Engineering Science*, 104, 800–812.
- [7] N. Gokon, T. Kodama, & Y. Kato, (2014). Solar methane reforming using molten salt heat transfer systems. *International Journal of Hydrogen Energy*, vol. 39 issue 29, pp. 16202–16210.
- [8] S. Ganguli, & M. Bhatt, (2023). A review of advanced reactor technologies for steam methane reforming. *Renewable and Sustainable Energy Reviews*, 173, 113095.
- [9] D. Dogo, M. Auta, & A. Abdulkareem, (2022). Modeling and simulation of steam methane reforming (SMR) process for hydrogen production. *International Journal of Engineering Processing & Safety Research*, vol 24, issue 5, pp. 161-172.
- [10] O. Massarweh, M. Al-khuzaei, M. Al-Shafi, Y. Bicer & A.S. Abushaikh, (2023). Blue Hydrogen Production from Natural Gas Reservoirs: A Review of Application and Feasibility. *Journal CO2 Utility* 70, 102438.
- [11] H. Ishaq, I. Dincer, C. A. Crawford, (2022). Review on Hydrogen Production and Utilization: Challenges and Opportunities. *International Journal of Hydrogen Energy*, 47, 26238–26264.
- [12] I. Staffell, D. Scamman, A. Velazquez Abad, P. Balcombe, P.E. Dodds, P. Ekins, N. Shah & K.R Ward, (2019). The Role of Hydrogen and Fuel Cells in the Global Energy System. *Energy Environmental Science*, 12, 463–491.
- [13] K. Bayramoğlu, (2024). Energy and Exergy Analysis of Diesel-Hydrogen and Diesel-Ammonia Fuel Blends in Diesel Engine. *Journal of Eta Maritime Science*. 12, 128–135.
- [14] N.S. Muhammed, A.O. Gbadamosi, E.I. Epelle, A.A. Abdulrasheed, B. Haq, S. Patil, D. Al-Shehri & M.S. Kamal, (2023) Hydrogen Production, Transportation, Utilization, and Storage: Recent Advances towards Sustainable Energy. *Journal of Energy Storage*, 73, 109207.
- [15] L. A. Bilgili, (2023). Systematic Review on the Acceptance of Alternative Marine Fuels. *Renew. Sustain. Energy Rev.* 182, 1133
- [16] J. R. Rostrup-Nielsen, J., Sehested, & J. K. Nørskov, (2002). Hydrogen and synthesis gas by steam- and CO<sub>2</sub> reforming. *Advances in Catalysis*, 47, 65–139.
- [17] S.Z. Abbas, V. Dupont, & T. Mahmud, (2017). Kinetics study and modelling of steam methane reforming process over a NiO/Al<sub>2</sub>O<sub>3</sub> catalyst in an adiabatic packed bed reactor. *International Journal of Hydrogen Energy* 42 (5), 2889-2903.